In Vivo Small Animal Imaging for Early Assessment of Therapeutic Efficacy of Photodynamic Therapy for Prostate Cancer

Baowei Fei [1,2,*], Hesheng Wang [2], Xiang Chen [1], Joseph Meyers [2], John Mulvihill [3], Denise Feyes [3], Nancy Edgehouse [4], Jeffrey L. Duerk, Thomas G. Pretlow [4], Nancy L. Oleinick [3]

Departments of Radiology [1], Biomedical Engineering [2], Radiation Oncology [3], and Pathology [4]
Case Western Reserve University, University Hospitals of Cleveland,
and the Case Comprehensive Cancer Center
* Corresponding Author: baowei.fei@case.edu.

ABSTRACT

We are developing *in vivo* small animal imaging techniques that can measure early effects of photodynamic therapy (PDT) for prostate cancer. PDT is an emerging therapeutic modality that continues to show promise in the treatment of cancer. At our institution, a new second-generation photosensitizing drug, the silicon phthalocyanine Pc 4, has been developed and evaluated at the Case Comprehensive Cancer Center. In this study, we are developing magnetic resonance imaging (MRI) techniques that provide therapy monitoring and early assessment of tumor response to PDT. We generated human prostate cancer xenografts in athymic nude mice. For the imaging experiments, we used a high-field 9.4-T small animal MR scanner (Bruker Biospec). High-resolution MR images were acquired from the treated and control tumors pre- and post-PDT and 24 hr after PDT. We utilized multi-slice multi-echo (MSME) MR sequences. During imaging acquisitions, the animals were anesthetized with a continuous supply of 2% isoflurane in oxygen and were continuously monitored for respiration and temperature. After imaging experiments, we manually segmented the tumors on each image slice for quantitative image analyses. We computed three-dimensional T2 maps for the tumor regions from the MSME images. We plotted the histograms of the T2 maps for each tumor pre- and post-PDT and 24 hr after PDT. After the imaging and PDT experiments, we dissected the tumor tissues and used the histologic slides to validate the MR images. In this study, six mice with human prostate cancer tumors were imaged and treated at the Case Center for Imaging Research. The T2 values of treated tumors increased by 24 ± 14% 24 hr after the therapy. The control tumors did not demonstrate significant changes of the T2 values. Inflammation and necrosis were observed within the treated tumors 24 hour after the treatment. Preliminary results show that Pc 4-PDT is effective for the treatment of human prostate cancer in mice. The small animal MR imaging provides a useful tool to evaluate early tumor response to photodynamic therapy in mice.

Keywords: Small animal imaging, photodynamic therapy, prostate cancer, magnetic resonance imaging, therapeutic assessment

1. INTRODUCTION

Photodynamic therapy (PDT) is a novel therapeutic modality for cancer treatment.[1] With PDT, a tumor-localized photosensitizer is irradiated with red light to generate reactive oxygen that efficiently kills cells and ablates tumors.[1] PDT can be administered deep into tumors using minimally invasive techniques as only the small laser fiber that delivers the light to the tumor needs to be inserted into the lesions. PDT with Photofrin is US-FDA approved for treating early and advanced lung cancer, advanced esophageal cancer, and Barrett's esophagus.[1,2] An important

Medical Imaging 2007: Physiology, Function, and Structure from Medical Images, edited by Armando Manduca, Xiaoping P. Hu, Proc. of SPIE Vol. 6511, 651102, (2007) · 1605-7422/07/$18 · doi: 10.1117/12.708718

advantage of PDT is that both the photosensitizer and the light are inert by themselves, and the light can be precisely focused onto a selected region, allowing extreme specificity in the localization of the photodynamic effect. Consequently, systemic toxicities are minimized.

Magnetic resonance imaging (MRI) techniques provide a useful tool for assessing PDT efficacy. First, MRI has been used to evaluate PDT-induced vascular damage followed by hemorrhagic necrosis in murine M1 tumors in mice.[3] Blood oxygenation level-dependent (BOLD) contrast MRI shows attenuation (25-40%) of MR signal at the treated tumor site.[4] Decreases in contrast agent uptake rates following PDT were observed by gadolinium-contrast MRI.[5] Second, *in vivo* ^{31}P nuclear magnetic resonance (NMR) spectroscopy has been used to monitor tumor metabolic status before and after the treatment of RIF-1 tumors [6,7] and mammary carcinoma.[8,9] The NMR data revealed significant differences in the time course of high energy phosphate levels in combined hyperthermia and photodynamic therapies.[8] It was also demonstrated that there is a relationship between NMR measurements immediately following PDT and the ultimate effect on the tumor.[7] Third, diffusion-weighted MRI showed a biphasic change in the apparent diffusion coefficient (ADC) within the first 24 hours post-PDT, indicating the early response of PC-14 tumors to PDT.[10]

In a previous study, we used both MRI and positron emission tomography (PET) to image C3H mice bearing RIF-1 tumors after PDT.[11-13] PET with ^{18}F-fluorodeoxyglucose (FDG) provided metabolic information of the tumors. High-resolution MRI provided anatomical and morphological changes of the lesions. Both rigid and deformable image registration methods were developed to combine MRI and PET images for improved tumor monitoring. Fusion of MRI and PET images provided both anatomical and functional information of the tumors for evaluating PDT effects. We found that the tumor FDG uptake decreased immediately after PDT.[11-13] In this study, we focus on small animal MR imaging and analysis methods for monitoring the efficacy of prostate PDT *in vivo*. To the best of our knowledge, this is the first report on *in vivo* imaging for Pc 4-based PDT for prostate cancer. We are developing quantitative image analysis techniques to identify the subtle changes immediately after PDT for evaluating therapeutic efficacy.

2. MATERIALS AND METHODS

2.1 Pc 4 formulation

The chemical synthesis of Pc 4 was described earlier [15]. A stock solution (1 mg/ml) was made by dissolving Pc 4 at 10 mg/ml in 50% Cremophor EL, 50% absolute ethanol, then adding 9 volumes of normal saline with mixing. For injection, the Pc 4 stock solution was mixed with an equal volume of 5% Cremophor EL, 5% ethanol. Each animal was weighed at the time of injection, and the volume of injected solution adjusted to give the desired dose in mg/kg.

2.2 PC-3 human prostate cancer model

Human prostate cancer PC-3 cells were grown as monolayers in E-MEM supplemented with 15% fetal bovine serum. Male athymic nude mice of 4-8 weeks old were obtained from the Case Comprehensive Cancer Center Athymic Animal Facility and housed under pathogen-free conditions. They were maintained under controlled conditions (12-h dark-light cycles; temperature 20-24˚C) with free access to sterilized mouse chow. Two tumors were initiated in each mouse by injection of 10^5 - 10^6 PC-3 cells intradermally on the shoulder flanks. One of the two tumors was treated and the other served as the control. Procedures involving animals and their care were conducted in conformity with the guidelines of the Institutional Animal Care and Use Committee.

2.3 Photodynamic therapy protocol

Tumors were treated and imaged when they reached 5-8 mm in diameter, which required 2-4 weeks after implantation. Animals were given Pc 4 (0.6 mg/kg) by tail-vein injection. We know from experience that neither the light nor the photosensitizer alone produces any response. After 48 hours, a 1-cm area encompassing the tumor was irradiated with red light (672 nm; 150 J/cm^2; 150 mW/cm^2) from a diode laser (Applied Optronics Corp., Newport) coupled to a fiber optic terminating in a microlens, which distributed light uniformly throughout the treatment field. One of the two tumors was exposed to red light and the other tumor in each animal served as a control (receiving photosensitizer but no light). To measure histologic responses following Pc 4-PDT, mice were sacrificed at different time points (immediately, 24 h, 48 h and 7 day) after therapy. The tumors were surgically removed and immediately stored in 10% formalin for 2-7 days before histologic processing.

2.4 Image acquisitions

Two days after photosensitizer injection, high-resolution MR images were acquired from each mouse pre- and post-PDT and 24 hour after PDT. The mouse MR images were acquired using a high-field (9.4-T) small animal MR scanner (Bruker BioSpin GmbH, Rheinstetten, Germany). A dedicated whole body mouse coil was used for the image acquisitions. A multi-slice multi-echo (MSME) sequence (TR=6929 ms and TE=28, 56, 84, and 111 ms) with a slice thickness of 0.5 mm was used to generate high-resolution coronal images (Matrix: 256 x 256, Pixel size: 0.27 x 0.13-mm). In these T2-weighted images, the tumors were clearly delineated by the bright subcutaneous fat signals.

2.5 Image processing and analysis

Using the commercial image software Analyze (AnalyzeDirect, Inc., Overland Park, KS), we manually segmented the tumor on each image slice from the MR image volumes. The segmented images were used for the calculation of T2 maps and tumor volumes. The four MSME images were used to generate the T2 maps over the tumor regions. We used the software package Paravision 3.1 (Bruker BioSpin GmbH, Rheinstetten, Germany) for the computation of T2 maps. Once we obtained the T2 values for each voxel within the tumor region, we calculated the histogram, mean, and standard deviation of the T2 values of the tumor.

3. RESULTS AND DISCUSSION

Figure 1 shows the MSME images of a treated tumor. The images were acquired pre- and post-PDT and 24 hours after PDT. From the MR images, signal changes within the treated tumor region were observed 24 hours after PDT. Figure 2 shows the corresponding T2 maps of the treated tumor calculated from the MSME images. From the T2 maps, the T2 values of the treated tumor increased 24 hours after PDT.

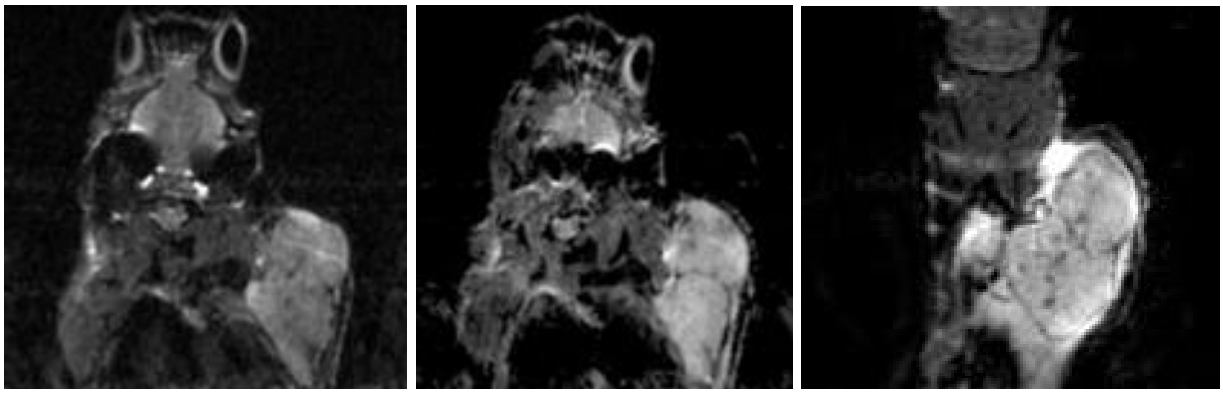

Figure 1. Multi-slice multi-echo (MSME) MR images of a treated tumor pre-PDT (left), immediately post-PDT (middle), and 24 hours after PDT (right). The signal intensity values changed 24 hours after the treatment.

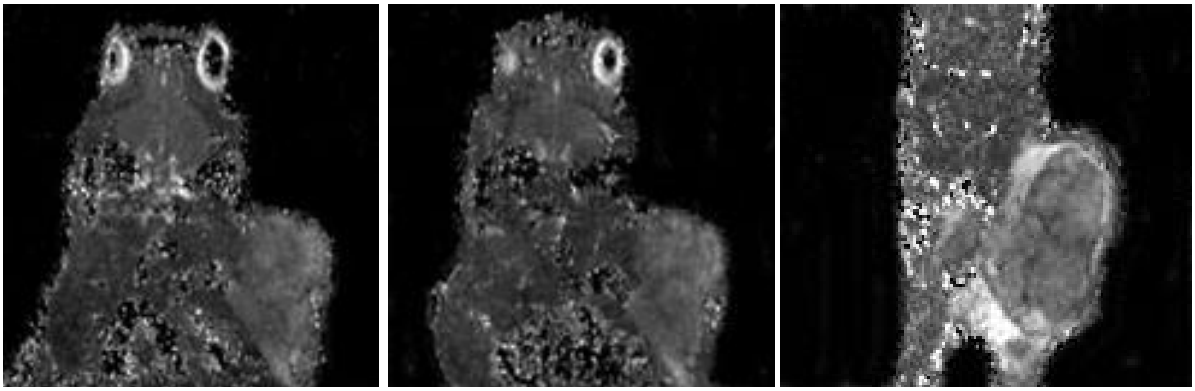

Figure 2. T2 maps of the treated tumor pre-PDT (left), immediately post-PDT (middle) and 24 hours after PDT (right). The MSME images as shown in Figure 1 were used to calculate the T2 maps. T2 values increased 24 hours after the treatment.

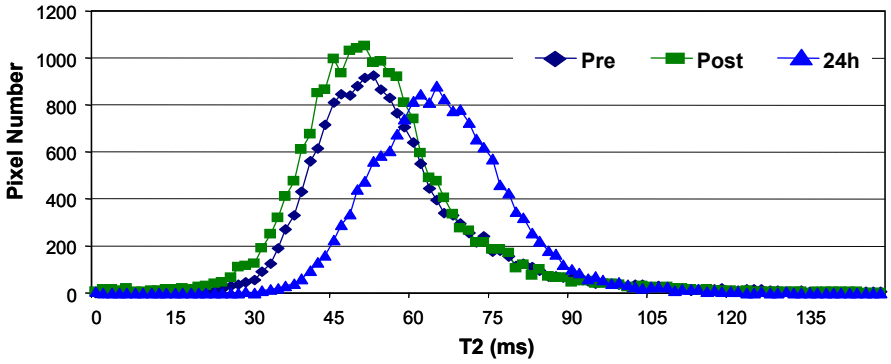

Figure 3. Histograms of the T2 maps pre- and post-PDT and 24 hours after PDT. The histogram curve shifted to the right 24 hours after the treatment, indicating the increases in the T2 values within the treated tumor.

Figure 3 shows the histograms of the T2 maps within the tumor region. The histogram shifted to the right 24 hours after PDT, indicating that the T2 values increased after the treatment. This is consistent with the observed signal changes on the MSMS images and the T2 maps. The mean T2 values are 56.1 ± 16.0 ms, 53.6 ± 15.7 ms, and 65.5 ± 13.1 ms pre-PDT, immediately post-PDT, and 24 hours post-PDT, respectively. Twenty-four hours after PDT, the mean T2 values increased by 17% for this typical mouse.

Figure 4 displays the T2 values of the treated and control tumors for six mice. For the treated tumors, the mean T2 values increased by 24 ± 14% 24 hours after PDT. There is a significant difference between the T2 values pre-PDT and 24 hours after PDT ($p=0.002$). For the control tumors, the T2 values increased by 6 ± 9%, indicating a non-significant difference between the T2-values of pre-PDT and 24 hours after PDT ($p=0.114$). Histologic slides showed that an inflammatory response with edema was observed in the treated tumor, which was not seen within the control tumor. This is consistent with the increases of the T2 values of the treated tumor tissues.

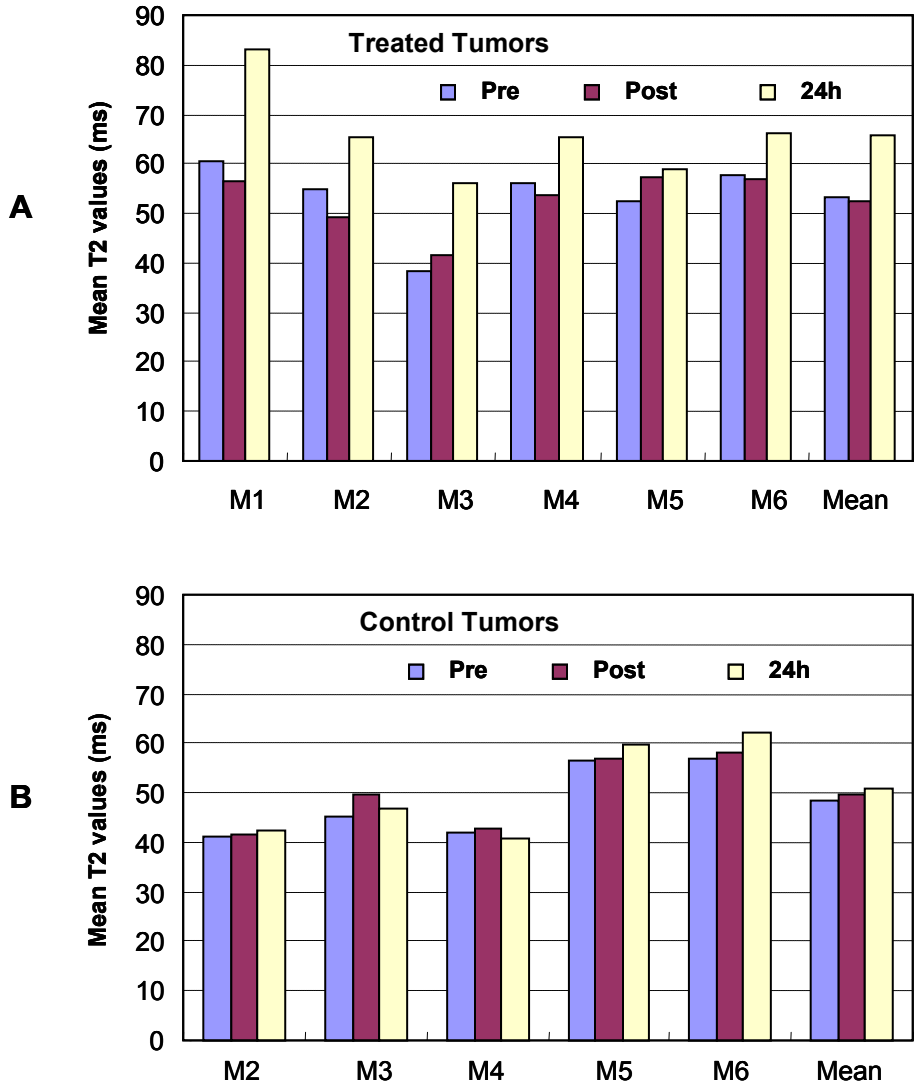

Figure 4. T2 values of the treated and control tumors for six mice (M1-M6). For the treated tumors, the mean T2 values are 53.4 ± 7.8 ms, 52.6 ± 6.2 ms, and 65.9 ± 9.4 ms pre-PDT, post-PDT, and 24 hours after PDT, respectively. For the control tumors, the mean T2 values are 48.4 ± 6.9 ms, 49.8 ± 6.9 ms, and 52.0 ± 11.2 ms pre-PDT, post-PDT, and 24 hours after PDT, respectively. Mouse M1 had only one tumor that was treated.

4. DISCUSSION AND CONCLUSION

We developed small animal MR imaging and analysis methods for assessing the efficacy of photodynamic therapy (PDT) of human prostate cancer growing as a xenograft in athymic nude mice. Our preliminary results show that high-resolution MR images can detect the early tumor response to the therapy 24 hours after the treatment. For treated tumors, the T2 values significantly increased one day after the treatment. For the control tumors, there was no significant difference between the T2 values before and 24 hours after the therapy. The MR parameters (T2 values) may provide a surrogate biomarker to predict the success of the therapy. This method could provide a powerful tool for other applications of small animal imaging in cancer biology, functional genomics, and drug development.

ACKNOWLEDGEMENTS

This work was partially supported by NIH grant R21CA120536 and a Case Comprehensive Cancer Center Pilot Award to Baowei Fei. The imaging facility is supported by the Northeastern Ohio Small Animal Imaging Resource Center, which is funded by NIH grant R24CA110943.

Reference List

1 T.J.Dougherty, "An update on photodynamic therapy applications," *J Clin.Laser Med Surg.*, vol. 20, pp. 3-7, Feb, 2002.

2 T.J.Dougherty, C.J.Gomer, B.W.Henderson, G.Jori, D.Kessel, M.Korbelik, J.Moan, and Q.Peng, "Photodynamic therapy," *J Natl.Cancer Inst.*, vol. 90, pp. 889-905, Jun 17, 1998.

3 B.G.Winsborrow, H.Grondey, H.Savoie, C.A.Fyfe, and D.Dolphin, "Magnetic resonance imaging evaluation of photodynamic therapy-induced hemorrhagic necrosis in the murine M1 tumor model," *Photochem.Photobiol.*, vol. 66, pp. 847-852, Dec, 1997.

4 S.Gross, A.Gilead, A.Scherz, M.Neeman, and Y.Salomon, "Monitoring photodynamic therapy of solid tumors online by BOLD-contrast MRI," *Nat.Med*, vol. 9, pp. 1327-1331, Oct, 2003.

5 S.D.Kennedy, L.S.Szczepaniak, S.L.Gibson, R.Hilf, T.H.Foster, and R.G.Bryant, "Quantitative MRI of Gd-DTPA uptake in tumors: response to photodynamic therapy," *Magn Reson Med*, vol. 31, pp. 292-301, Mar, 1994.

6 J.Mattiello, J.L.Evelhoch, E.Brown, A.P.Schaap, and F.W.Hetzel, "Effect of photodynamic therapy on RIF-1 tumor metabolism and blood flow examined by 31P and 2H NMR spectroscopy," *NMR Biomed*, vol. 3, pp. 64-70, Apr, 1990.

7 J.C.Bremner, S.R.Wood, J.K.Bradley, J.Griffiths, G.E.Adams, and S.B.Brown, "31P magnetic resonance spectroscopy as a predictor of efficacy in photodynamic therapy using differently charged zinc phthalocyanines," *Br.J Cancer*, vol. 81, pp. 616-621, Oct, 1999.

8 Q.Jiang, M.Chopp, and F.W.Hetzel, "In vivo 31P NMR study of combined hyperthermia and photodynamic therapies of mammary carcinoma in the mouse," *Photochem.Photobiol.*, vol. 54, pp. 795-799, Nov, 1991.

9 Y.H.Liu, R.M.Hawk, and S.Ramaprasad, "In vivo relaxation time measurements on a murine tumor model--prolongation of T1 after photodynamic therapy," *Magn Reson Imaging*, vol. 13, pp. 251-258, 1995.

10 V.Plaks, N.Koudinova, U.Nevo, J.H.Pinthus, H.Kanety, Z.Eshhar, J.Ramon, A.Scherz, M.Neeman, and Y.Salomon, "Photodynamic therapy of established prostatic adenocarcinoma with TOOKAD: a biphasic apparent diffusion coefficient change as potential early MRI response marker," *Neoplasia.*, vol. 6, pp. 224-233, May, 2004.

11 B.W.Fei, H.Wang, R.F.Jr.Muzic, C.Flask, D.L.Wilson, J.L.Duerk, D.K.Feyes, and N.L.Oleinick, "Deformable and rigid registration of MRI and microPET images for photodynamic therapy of cancer in mice," *Medical Physics*, vol. 33, pp. 753-760, 2006.

12 B.W.Fei, R.Muzic, Z.Lee, C.Flask, R.Morris, J.L.Duerk, and D.L.Wilson, "Registration of micro-PET and high resolution MR images of mice for monitoring photodynamic therapy,"*Proceeding of SPIE on Medical Imaging: Physiology, Function, and Structure from Medical Images*,pp. 371-379, 2004.

13 B.Fei, H.Wang, R.F.Muzic, C.Flask, N.L.Oleinick, D.L.Wilson, and J.L.Duerk, "Finite Element Model-based Deformable Registration of microPET and High-resolution MR Images for Photodynamic Therapy in Mice,"*Medical Imaging 2006: Physiology, Function, and Structure from Medical Images*, edited by Amir A. Amini, Armando Manduca, Proceedings of SPIE,2006.

14 D.Lapointe, N.Brasseur, J.Cadorette, C.La Madeleine, S.Rodrigue, J.E.van Lier, and R.Lecomte, "High-resolution PET imaging for in vivo monitoring of tumor response after photodynamic therapy in mice," *J Nucl Med*, vol. 40, pp. 876-882, May, 1999.

15 N.L.Oleinick, A.R.Antunez, M.E.Clay, B.D.Rihter, and M.E.Kenney, "New phthalocyanine photosensitizers for photodynamic therapy," *Photochem.Photobiol.*, vol. 57, pp. 242-247, Feb, 1993.

Baowei Fei, Hesheng Wang, Xiang Chen, Joseph Meyers, John Mulvilhill, Denise Feyes, Nancy Edgehouse, Jeffrey L. Duerk, Thomas G. Pretlow, and Nancy L. Oleinick, “In vivo small animal imaging for early assessment of therapeutic efficacy of photodynamic therapy for prostate cancer”, Armando Manduca, Xiaoping P. Hu, Proc. SPIE 6511, 651102 (2007)

http://dx.doi.org/10.1117/12.708718